

Surface-State-Mediated Photochemistry: Laser-Induced Desorption of NO from Si(111)

Lee J. Richter, Steven A. Buntin, David S. King, and Richard R. Cavanagh

*Center for Atomic, Molecular, and Optical Physics, National Institute of Standards and Technology,
Gaithersburg, Maryland 20899*

(Received 26 April 1990)

Laser-induced desorption of NO from Si(111) has been investigated using state-specific detection techniques. Characterization of the internal-state population distributions with desorption-laser wavelengths in the range 1907–355 nm indicate that, at low initial NO coverages, desorption is driven by a common, nonthermal mechanism. The wavelength dependence of the yield and the effects of coadsorbates on the yield establish that photogenerated holes in a Si intrinsic surface state mediate the laser-adsorbate interaction.

PACS numbers: 82.65.-i, 73.20.-r, 78.90.+t, 82.50.-m

A wide variety of chemical processes at semiconductor surfaces have been observed to be promoted by radiation. The possible mechanisms for the transfer of the initial photon energy to the reaction coordinates are many, ranging from simple substrate heating effects to localized photoexcitations of adsorbates. In the case of above-band-gap radiation, reaction has often been attributed to the generation of chemically active surface species due to capture of photogenerated carriers.¹ State-resolved studies of laser-induced reaction products have proven extremely illuminating as they often allow the distinction and quantification of various competing excitation mechanisms.^{2,3} In this Letter we report a quantum-state-specific study of laser-induced desorption (LID) of NO from Si(111). The initial coverage⁴ of NO is kept sufficiently small [≈ 0.06 ML (monolayer), where $1 \text{ ML} \equiv 7.83 \times 10^{14} \text{ cm}^{-2}$] that the 7×7 reconstruction is still present. At these low NO coverages, we establish that the desorption is not driven by direct interaction with bulk carriers but is due to an interaction with photogenerated holes in an intrinsic surface state of the 7×7 reconstruction.

The experimental apparatus and principal procedures have been described earlier.² The samples were cut from 300- μm -thick wafers; both 1.5- Ωcm , B-doped p -type and 0.5- Ωcm , P-doped n -type substrates were used. Specimens were cleaned via Ne^+ -ion bombardment followed by thermal annealing at ≈ 950 K, a treatment which produces the 7×7 reconstruction as evidenced by sharp, bright seventh-order low-energy electron-diffraction (LEED) spots. NO exposures via a directed array were performed with the substrate at ≈ 100 K and controlled to give ≈ 0.06 ML coverage, resulting in a surface which is occupied by a single molecular NO species, and possibly some dissociation products.⁵ This low NO coverage resulted in no detectable degradation of the LEED pattern. Temperature programmed desorption (TPD) and Auger electron spectroscopy (AES) studies of this NO coverage indicate that the principal thermal reaction is dissociation. Simultaneous desorption of NO and N_2 occurs near 150 K as a minor reac-

tion channel; the ratio of desorbed $\text{NO}:\text{N}_2$ is $< 0.2:1$. AES indicates that dissociation also is the major photoreaction; however, LID studies detected via electron-impact-ionization mass spectroscopy indicate a significant increase in the ratio of photodesorbed NO to N_2 ($\text{NO}:\text{N}_2 \approx 1:1$) compared to the dark reaction.

The desorption-laser pulse was derived from a Q -switched Nd^{+3} -doped yttrium-aluminum-garnet (YAlG) laser and was incident normal to the crystal surfaces. The laser output at 1064 nm (1.16 eV) had a nearly Gaussian temporal profile with a 24-ns FWHM. Desorption-laser wavelengths of 1907 nm (0.65 eV), 1543 nm (0.80 eV), 532 nm (2.33 eV), and 355 nm (3.50 eV) were obtained by Raman shifting the fundamental or harmonic generation. Up to nine spots, equally spaced on a 2-mm grid, were irradiated with a 1-mm FWHM beam following a given surface preparation. After irradiation the substrate was subjected to an ion-sputter-thermal-anneal cycle to restore surface cleanliness and order. The radiation exposure on any given spot was usually limited to produce no more than a 10% decrease in the observed NO photodesorption yield. Typical pulse energies at 1064–355 nm were 0.4–3.0 μJ , while pulse energies of 0.3–1.0 mJ were used at 1907 and 1543 nm. Calculated laser-induced surface temperature rises are < 1 K for wavelengths ≤ 1064 nm. With a conservative estimate of 1% absorption of the sub-band-gap light, the 1543- and 1907-nm pulses generate no more than an 8-K bulk temperature increase.

The desorbed NO was detected with quantum-state resolution by laser-induced fluorescence (LIF) as described previously.² Kinetic-energy distributions for a specific internal state (vibration v , spin orbit Ω , rotation J) were extracted from optically detected time-of-flight (TOF) spectra obtained by varying the time delay between the firing of the desorption- and probe-laser pulses. We report flux-weighted average kinetic energies $\langle E_k \rangle / 2k$ derived from the spectra.²

The inset in Fig. 1 displays a typical TOF spectrum for $\text{NO}(v=0, \Omega = \frac{1}{2}, J=8.5)$ following desorption from an n -type sample with 1064-nm radiation; the $\langle E_k \rangle / 2k$

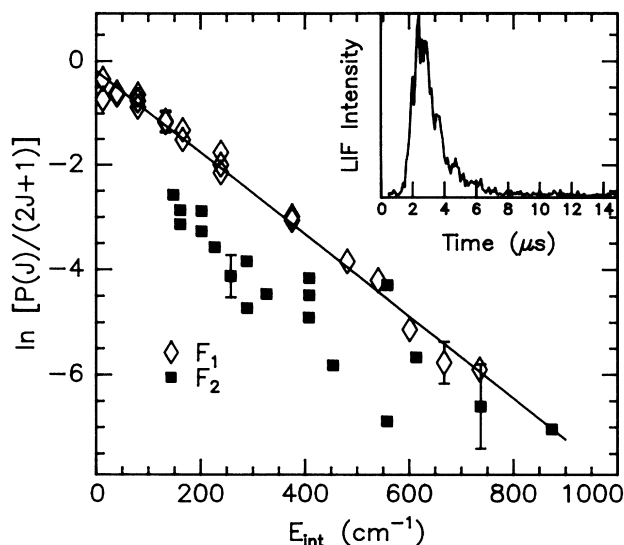


FIG. 1. Internal-state populations for LID of $\text{NO}(v=0)$ vs $E_{\text{int}} \equiv E_{\text{rot}} + E_n$. The desorption-laser wavelength was 1064 nm; the substrate was n -type Si(111). Inset: Time-of-flight spectrum for $\text{NO}(v=0, F_1, J=8.5)$ detected at a flight distance of 2.4 mm. Again, the incident light was 1064 nm, the substrate n type.

for the displayed spectrum is 760 K. The derived $\langle E_k \rangle / 2k$ were dependent on the quantum state probed, increasing monotonically from 670 to 1100 K as rotational energy E_{rot} increases from 40 to 735 cm^{-1} . The velocity distributions are substantially narrower than a Maxwell-Boltzmann distribution at large E_{rot} . At all desorption-laser wavelengths except 1907 nm, the fluence dependence of the desorption yield was studied over at least an order of magnitude range for selected quantum states and was found to be linear. The kinetic-energy distributions were independent of fluence. (Limited signal prohibited a study of the fluence dependence at 1907 nm.)

We present internal-state distributions derived from time integrals of TOF spectra due to the variations of the velocity distributions with internal state. The internal-state distributions for $\text{NO}(v=0)$ following desorption from an n -type sample with 1064-nm light are shown in Fig. 1, in the form of a Boltzmann plot. The data for the ground spin-orbit (F_1 , $\Omega = \frac{1}{2}$) states clearly lie on a common line, indicating that the rotational-level population distribution can be described by a Boltzmann distribution with a phenomenological rotational temperature T_r of 184 K.⁶ There is a significant selection for desorption into the F_1 spin-orbit state. The ratio of spin-orbit-state populations, F_1/F_2 (F_2 , $\Omega = \frac{3}{2}$), integrated over all rotational levels is 9 ± 1 . Within the limited signal, the rotational-level population distribution for the F_2 states is not significantly different from that given by the F_1 states.

The qualitative and quantitative aspects of the internal-state distributions for $\text{NO}(v=0)$ showed re-

markably little dependence on either desorption-laser wavelength or substrate doping. All aspects of the distributions for 1064-, 532-, and 355-nm light on n - and p -type samples were indistinguishable. For 1907- and 1543-nm radiation on p -type samples, the qualitative variation of the kinetic-energy distributions with E_{rot} , the Boltzmann nature of the F_1 states, and the selectivity for the F_1 states are the same. However, T_r was slightly cooler at 1543 and 1907 nm, ≈ 115 K. The insensitivity of the internal-state distributions to wavelength for the YAG harmonics establishes that a single desorption mechanism is responsible over the range 1064–355 nm. The qualitative similarity of the internal-state distributions for 1543 and 1907 nm suggests that the same mechanism is responsible for the entire range 1907–355 nm.

We have characterized the desorption-laser-wavelength dependence of the yield per incident photon for $\text{NO}(v=0)$ arising from this common mechanism. The yield was determined from the yield for select F_1 rotational levels, adjusted by the relative fractional populations determined from the measured internal-state distributions. On the p -type sample, the yields for 1907-, 1543-, 532-, and 355-nm radiation relative to that at 1064 nm were $1.4(\pm 0.3) \times 10^{-4}$, $7(\pm 3) \times 10^{-3}$, $9(\pm 3) \times 10^{-1}$, and $15(\pm 2)$. The wavelength dependence of the yield (determined from the yields for 532 and 355 nm, relative to that of 1064 nm on n -type material) is independent of substrate doping. The uncertainty in determinations of the ratio of the absolute yield from n - and p -type samples is at least a factor of 2 since the optical components must be disturbed during bake-out of the chamber after changing samples. The LIF signal for NO desorbed from p -type samples was ≈ 0.2 times that from n -type samples for wavelengths 1064–355 nm, establishing that the absolute yield from p - and n -type samples is of comparable magnitude.

The negligible laser-induced temperature jump, the linear fluence dependence of the yield, and the independence of the kinetic-energy distributions on fluence eliminate thermal effects and establish that the desorption mechanism is truly photochemical. In earlier work,⁷ it was proposed that the photodesorption of NO from Si(111) at high coverages (saturation) was driven by photogenerated hot carriers. The indirect gap at 100 K is 1.15 eV; therefore 1064-nm photons produce carriers with only 15 meV excess energy. The significant yield we observe for LID of NO with 1064-nm incident light clearly rules out mechanisms involving hot photogenerated carriers at low initial coverages. We find that as the NO coverage is increased above ≈ 0.12 ML, the low-coverage channel is quenched. An NO -saturated surface displays a desorption channel with distinctly different internal-state distributions which are strongly dependent on desorption-laser wavelength, supporting the conclusion that the excitation mechanism changes with coverage.⁸

Our observations also rule out mechanisms involving only "thermalized" (band-edge) carriers. Inconsistencies exist between the expected thermalized carrier transport, based on numerical solutions of the drift-diffusion equations, accounting for realistic rates of surface recombination and band bending,⁹ and our data. First, the absorption depth of both 532- and 355-nm radiation is sufficiently short¹⁰ that the spatial distribution of thermalized photocarriers is determined by their diffusion during the laser pulse and not the absorption coefficient. Therefore, both the carrier temporal and spatial profiles for these two wavelengths are identical and a process driven by a thermalized carrier would have relative photodesorption yields, (532 nm)/(355 nm), given by the relative optical absorption: $0.63/0.42 = 1.5$; however, the observed relative yield was ≈ 0.1 . Second, in contrast to the shorter wavelengths, the absorption of 1064-nm light at 100 K is very weak:¹¹ $\alpha < 0.1 \text{ cm}^{-1}$. For the fluences used ($\approx 5 \text{ kW/cm}^2$) at 1064 nm, the absorption is insufficient to flatten the bands if they are assumed to be bent by their clean-surface values of $\approx 0.5 \text{ eV}$.¹² Therefore, the yield due to a single band-edge carrier would be negligible for one of either *n*-type or *p*-type doping; however, the yields for the two types of doping were comparable.

Since the observed desorption is not related to the generation of bulk carriers, we propose that the desorption arises from excitations in the intrinsic surface states of the 7×7 reconstructed Si(111).^{13,14} This mechanism is immediately suggested by the observation of desorption with sub-band-gap radiation (0.80 and 0.65 eV). There are three, broad (the widths of these states are $\approx 0.4 \text{ eV}$ ¹³), surface states accessible to all wavelengths studied: the S_2 state, a band of doubly occupied dangling bonds on the rest atoms centered $\approx 0.2 \text{ eV}$ below the valence-band maximum; the S_1 state, a partially occupied band of dangling bonds localized on the adatoms and centered in the band gap; and the S state, an unoccupied band of dangling bonds, again localized on the adatoms, near the conduction-band minimum. It is unlikely that excitations in the S_1 band are responsible for the desorption, as both electrons and holes are present in the band in the dark. However, participation of either the S_2 or S states appear consistent with the observed yield over the 1907–355-nm wavelength range. The S_1 state can act as a source for photoinjection of electrons into the S band and holes into the S_2 band at wavelengths $> 1064 \text{ nm}$ and transitions between bulk states and the S_2 and S states should occur for wavelengths $\lesssim 1064 \text{ nm}$.

Desorption via excitation of a surface state is further supported by the sensitivity of the LID to coadsorbed species on the surface. A series of coadsorption experiments were performed with species whose effects on the various surface states are well established. Exposure of low coverages of NO to saturation doses of N_2O resulted in no change in either the NO LID yield or the inter-

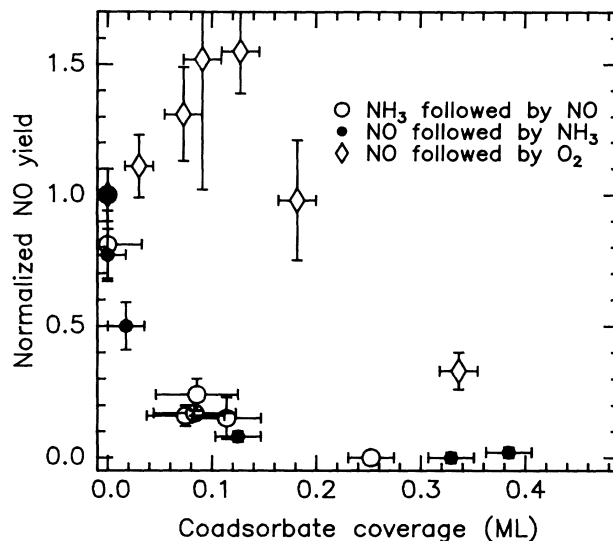


FIG. 2. Yield for $\text{NO}(v=0)$ following coadsorption of either O_2 or NH_3 , relative to the yield with no coadsorbates. The coverage of NH_2 or O was determined by AES following TPD of the NO . The initial NO coverage, determined from AES and TPD, was 0.06 ML. The desorption-laser wavelength was 1064 nm; the substrate was *p*-type Si(111). Similar behavior is observed on *n*-type Si(111) at both 1064 and 355 nm.

nal-state distributions. Adsorption of N_2O selectively quenches the adatom S_1 state,¹⁵ implying that neither the adatom-localized S_1 state nor, presumably, the adatom-localized S state is important to the low-coverage LID channel. NH_3 dissociatively adsorbs as NH_2 and H , preferentially bonding to rest atoms at low coverages, quenching the S_2 state.¹⁶ The NO LID yield, determined from selected internal states as described earlier, for NO coadsorbed with NH_3 is shown in Fig. 2. NH_3 exposures quenched the yield, but did not alter the internal-state distributions significantly, implying that the S_2 state is involved in the LID. The importance of the S_2 state and irrelevance of the adatom states (S and S_1) is supported by the effects of the coadsorption of O_2 , also shown in Fig. 2. Exposures of O_2 initially did not quench the low-coverage NO LID; however, higher O_2 exposures did result in a decreased yield. The adsorption of O_2 initially quenches the S_1 state, and subsequently quenches the S_2 state.¹⁷

The coadsorption studies indicate that the LID requires the presence of a S_2 hole. The preceding discussion of the role of hot and thermalized carriers rules out desorption driven by bulk carriers resulting from the creation of S_2 holes. The requirement of a S_2 hole accounts for the quenching of the low-coverage LID channel at high NO coverages. Photoemission studies indicate that, like O_2 , NO preferentially quenches the S_1 state at low coverage and quenches both the S_1 and S_2 states at saturation.¹⁵ Desorption via creation of S_2 holes also accounts for the independence of the internal energy distributions on desorption-laser wavelength as a

common excitation is created at all wavelengths.

There are at least two possible mechanisms by which the S_2 hole itself could promote NO desorption. Charge transfer occurs between the S_1 and S_2 states on the clean surface.^{14,16} If the low-coverage NO forms a covalent bond with an adatom via sharing of their respective unpaired electrons, consistent with the observation¹⁵ that NO initially quenches the S_1 state, then transfer of one of those bonding electrons to the photogenerated S_2 hole could weaken the chemisorption bond and lead to desorption. An alternate mechanism for photostimulated processes has been put forth by Weeks, Tully, and Kimerling in the context of explaining recombination-enhanced diffusion.¹⁸ In their model, localized lattice excitations created during carrier recombination results in efficient coupling of electronic energy into chemical reactions. Neutralization of the S_2 hole could generate lattice excitations sufficiently localized to the surface to induce desorption. Our measured internal-state distributions will provide a stringent test for future detailed dynamical calculations based on either desorption mechanism.

In summary, state-specific measurements of the LID of NO from low initial coverages have established that the process can be described by a single, nonthermal desorption mechanism over the desorption-wavelength range 1907–355 nm. The desorption is mediated by the presence of excitations in the intrinsic surface states of the substrate. Excitation of surface states should prove to be important to general systems where they are present, and may represent an opportunity for unique nonthermal processing.

This work was partially supported by the U.S. Department of Energy, Office of Basic Energy Sciences (D.E.-AI05-84ER13150). We thank Dr. F. Bozso and Dr. Ph. Avouris for communication of their results prior to publication.

¹S. R. Morrison, *The Chemical Physics of Surfaces* (Plenum, New York, 1977).

²S. A. Buntin, L. J. Richter, R. R. Cavanagh, and D. S.

King, *Phys. Rev. Lett.* **61**, 1321 (1988); *J. Chem. Phys.* **91**, 6429 (1989); L. J. Richter, S. A. Buntin, R. R. Cavanagh, and D. S. King, *J. Chem. Phys.* **89**, 5344 (1988).

³J. A. Prybyla, T. F. Heinz, J. A. Misewich, M. M. T. Loy, and J. H. Glowina, *Phys. Rev. Lett.* **64**, 1537 (1990); E. Hasselbrink, S. Jakubith, S. Nettesheim, M. Wolf, A. Cassuto, and G. Ertl, *J. Chem. Phys.* **92**, 3154 (1990); E. P. Marsh, T. L. Gilton, W. Meier, M. R. Schneider, and J. P. Cowin, *Phys. Rev. Lett.* **61**, 2725 (1988); F. A. Houle, *Phys. Rev. Lett.* **61**, 1871 (1988).

⁴NO coverages were determined by Auger electron spectroscopy and temperature programmed desorption.

⁵Z. C. Ying and W. Ho, *J. Chem. Phys.* **91**, 2689 (1989).

⁶All reported T , have an estimated accuracy of 10%.

⁷Z. Ying and W. Ho, *Phys. Rev. Lett.* **60**, 57 (1988).

⁸L. J. Richter, S. A. Buntin, D. S. King, and R. R. Cavanagh (to be published).

⁹Modeling was performed with PC-1D, available from Iowa State University Extension Software Service. Validity of the use of the drift-diffusion equations for modeling carrier transport during ns laser irradiation was recently provided by J. P. Long, H. R. Sadeghi, J. C. Rife, and M. N. Kabler, *Phys. Rev. Lett.* **64**, 1158 (1990).

¹⁰D. E. Spnes and A. A. Studna, *Phys. Rev. B* **27**, 985 (1983).

¹¹G. G. Macfarlane, T. P. McLean, J. E. Quarrington, and V. Roberts, *Phys. Rev.* **111**, 1245 (1958).

¹²J. E. Demuth, W. J. Thompson, N. J. DiNardo, and R. Imbihl, *Phys. Rev. Lett.* **56**, 1408 (1986); F. J. Himpsel, G. Hollinger, and R. A. Pollak, *Phys. Rev. B* **28**, 7014 (1983).

¹³R. J. Hamers, R. M. Tromp, and J. E. Demuth, *Surf. Sci.* **181**, 346 (1987); P. Mårtensson, W.-X. Ni, G. V. Hansson, J. M. Nicholls, and B. Reihl, *Phys. Rev. B* **36**, 5974 (1987); R. I. G. Uhrberg, G. V. Hansson, J. M. Nicholls, P. E. S. Persson, and S. A. Flodström, *Phys. Rev. B* **31**, 3805 (1985).

¹⁴J. E. Northrup, *Phys. Rev. Lett.* **57**, 154 (1986).

¹⁵F. Bozso and Ph. Avouris (to be published).

¹⁶Ph. Avouris and R. Wolkow, *Phys. Rev. B* **39**, 5091 (1989); F. Bozso and Ph. Avouris, *Phys. Rev. B* **38**, 3987 (1988).

¹⁷G. V. Hansson, R. I. G. Uhrberg, and S. A. Flodström, *J. Vac. Sci. Technol.* **16**, 1287 (1979); U. Höfer, A. Puschmann, D. Coulman, and E. Umbach, *Surf. Sci.* **211/212**, 948 (1989); A. J. Schell-Sorokin and J. E. Demuth, *Surf. Sci.* **157**, 273 (1985).

¹⁸J. D. Weeks, J. C. Tully, and L. C. Kimerling, *Phys. Rev. B* **12**, 3286 (1975).